

Virtual Serial Power Split Strategy for Parallel Hybrid Electric Vehicles

Alfonso Pantoja-Vazquez¹, Guillermo Becerra², Luis Alvarez-Icaza³
Instituto de Ingeniería - Universidad Nacional Autónoma de México
Coyoacán, D.F. 04510, México

Abstract—A new strategy for hybrid electric vehicles power flow control is presented. The strategy takes advantage of the kinematic and dynamic constraints of a planetary gear system used to couple the internal combustion engine and the electric machine. With this coupling, the strategy is able, most of the time, to operate the engine at maximum efficiency and to keep the battery state of charge on the desired level by making use of a easy to tune PI controller. The computational requirements of the strategy are low. Although the strategy is not proven optimal, it is inspired on optimal control theory.

I. INTRODUCTION

Concern on the use of fossil fuel is an important matter for today's society since it is a nonrenewable resource and because of the associated issues, like global warming and socio-economical problems. The reduction of the human transportation impact on energy consumption has been a challenge for governments, industry and researchers on the last years (Gong *et al.*, 2008; Schouten *et al.*, 2002).

Hybrid Electric Vehicles (HEV) are an option to help solving this problem. They use a combination of two or more power sources, usually an Internal Combustion Engine (ICE) and an Electric Machine (EM). HEV can reduce energy consumption and pollutant emissions compared to conventional vehicles due to the extra degree of freedom added by the EM, and also due to the ability of regenerative braking. All of these benefits are available, without sacrificing the conventional vehicle's attributes like performance, safety and reliability. These benefits also implies that the performance of the Hybrid Electric Vehicles (HEV) is strongly related to the power split strategy (Lin *et al.*, 2003; Musardo *et al.*, 2005; Sciarretta *et al.*, 2004).

In the literature several design approaches have been proposed for power split strategies. Some of them based on heuristics approaches, like fuzzy logic are presented in (Langari y Won, 2003; Schouten *et al.*, 2002), fuzzy logic tunned with genetic algorithms in (Zhang *et al.*, 1997) and rule based strategies optimized with Dynamic Programming (DP) in (Lin *et al.*, 2002; Lin *et al.*, 2003). Some approaches based on optimal control theory can be found in (Delprat *et al.*, 2001; Delprat *et al.*, 2004; Kessels *et al.*, 2008). The Equivalent Consumption Minimization Strategy (ECMS) is presented in (Sciarretta *et al.*, 2004; Zhang *et al.*, 2010) and

a predictive control is described in (Borhan *et al.*, 2009). There are also approaches based on DP or that use DP to tune the proposed strategy (Johannesson y Egardt, 2008; Lin *et al.*, 2003; van Keulen *et al.*, 2010). Although DP achieves an optimal solution, it is not suitable for online implementation because of the dependence on the future driving conditions. On the other hand, strategies based on ECMS are causal, but their performance may vary depending on the driving cycle (Zhang *et al.*, 2010). More recently, a new strategy has been proposed in (Becerra *et al.*, 2011) for parallel HEV. This strategy takes advantage of the kinematic and dynamic constraints from a Planetary Gear System (PGS) used as the mechanical coupling between the ICE and the EM. These constraints give one more degree of freedom from the power split strategy point of view.

Similar to the strategy presented in (Becerra *et al.*, 2011), the present work takes advantage of the PGS as the mechanical coupling device between the ICE and the EM. Using the kinematic constraint on the PSG, the ICE power is kept on its most efficient operation point, almost all the time, and the EM receives the excess or delivers the lack of power in order to achieve the power required in the driving cycle. By itself, this strategy tends to deplete or fill in the battery, depending on the driving cycle, To avoid this, a PI controller is added to adjust the ICE power when the battery State Of Charge (SOC) is different to its reference.

The rest of this paper is organized as follows. In the second section, the model and configuration used for simulations of the HEV are presented; in the third section, the problem is formulated and the *virtual serial strategy* is presented; simulation results of the proposed strategy over several driving cycles and its parameter robustness is analyzed in the fourth section; finally, conclusions and future work are presented in the fifth section.

II. HYBRID VEHICLE MODEL

The configuration selected in this work is a parallel one, where the ICE and the EM are coupled via a PGS, see Fig. 1, as proposed in (Becerra *et al.*, 2011). The complete model is simulated in ADVISOR (Markel *et al.*, 2002; Gao *et al.*, 2007).

A. Vehicle Model

The power requested by the power train P_p is calculated by modeling the vehicle like a moving mass subject to a

¹ apantojav@iingen.unam.com

² gbecerran@iingen.unam.com

³ alvar@pumas.iingen.unam.mx

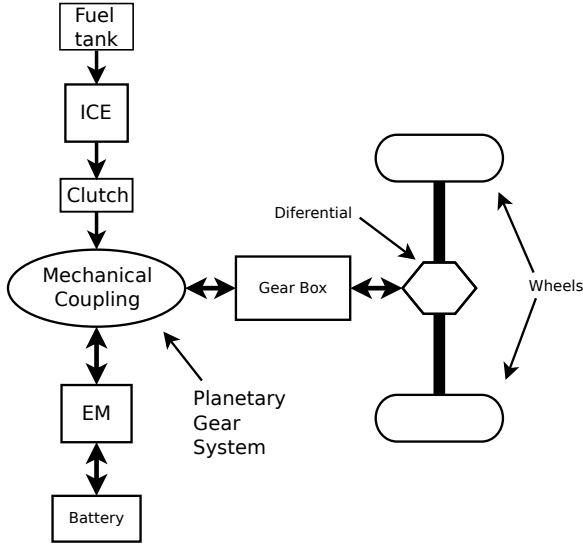


Fig. 1. Parallel HEV configuration.

traction force F_{tr} , provided by the power sources (Becerra *et al.*, 2011). The vehicle velocity dynamic $v(t)$ is

$$m \frac{dv(t)}{dt} = F_{tr} - \frac{1}{2} \rho_a C_d A_d v(t)^2 - mg C_r \cos(\gamma(t)) - mg \sin(\gamma(t)) \quad (1)$$

where ρ_a is the air density, C_d is the aerodynamic drag coefficient, A_d is the vehicle frontal area, m is the vehicle mass including the cargo mass, g is the gravity acceleration constant, C_r is the tire rolling resistance coefficient and $\gamma(t)$ is the road slope.

The torque and speed requested by the power train, τ_p and ω_p , respectively are

$$\omega_p = \frac{R_f}{R_w} R(t) v(t) \quad (2)$$

$$\tau_p = \frac{R_w}{R_f} \frac{1}{R(t)} F_{tr} \quad (3)$$

where $R(t)$ is the gearbox ratio, R_f is the final drive ratio and R_w is the wheel radius.

Finally, the power requested by the power train is

$$P_p(t) = \omega_p(t) \tau_p(t) = v(t) F_{tr}(t) + P_{acc} \quad (4)$$

where P_{acc} is the power required by the vehicle accessories.

B. ICE Model

The ICE is modeled through a static nonlinear map, taken from ADVISOR, which relates the ICE fuel rate consumption \dot{m}_f , with the torque at the crankshaft τ_{ice} and the engine speed ω_{ice} , in other words

$$\dot{m}_f = f(\omega_{ice}, \tau_{ice}) \quad (5)$$

Using the fuel Lower Heat Value, the ICE efficiency map is generated, Fig. 2 shows the map for the ICE used on this work. From this point of view, when the ICE is operating,

it is desired to operate it on the most efficient points of the map.

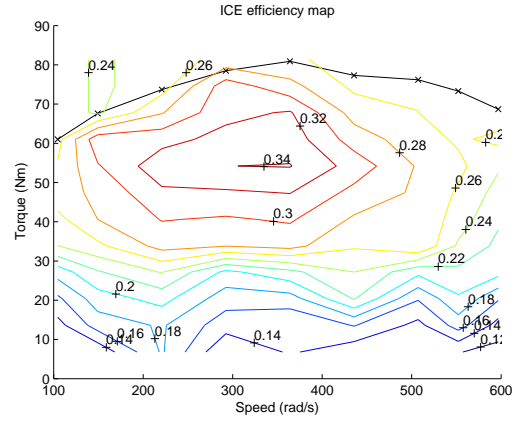


Fig. 2. ICE efficiency map.

C. EM Model

In an HEV the EM can work as motor or as generator depending if it is required to give or receive energy. EM is modeled also using a static nonlinear map which relates the EM speed ω_{em} and EM torque τ_{em} with an efficiency when it works as generator η_{gen} , and another one when it works as motor η_{mot} .

In other words, if the EM works as motor, $\tau_{em} \geq 0$, then

$$P_{em} = \eta_{mot}(\tau_{em}, \omega_{em}) P_{bat} \quad (6)$$

or if it works as generator, $\tau_{em} < 0$, then

$$P_{bat} = \eta_{gen}(\tau_{em}, \omega_{em}) P_{em} \quad (7)$$

with $P_{em} = \tau_{em} \omega_{em}$ and P_{bat} is the electric power.

D. Battery

The battery is modeled like a voltage source v_{oc} with an internal resistance R_{int} which depends on the SOC. The equivalent circuit is shown in Fig. 3, where v_{oc} is the battery's open circuit voltage, i_{bat} is the bus current and v_{bat} is the bus voltage.

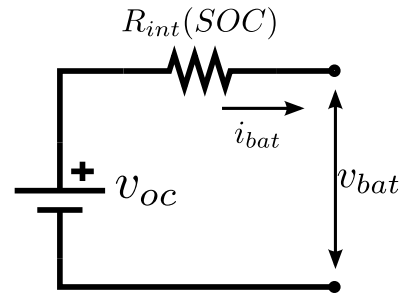


Fig. 3. Battery equivalent circuit.

Using the Kirchoff's voltage law, i_{bat} is found by solving

$$R_{int}(SOC)i_{bat}^2 - v_{oc}i_{bat} + P_{bat} = 0 \quad (8)$$

and v_{bat} is

$$v_{bat} = v_{oc} - R_{int}(SOC)i_{bat} \quad (9)$$

Finally, the SOC percentage is obtained from the expression (Becerra *et al.*, 2011)

$$SOC(t) = \min \left\{ 100, \max \left\{ 0, 100 \frac{Q_0 - \int_{t_0}^t i_{bat}(\tau) d\tau}{Q_T} \right\} \right\} \quad (10)$$

where Q_0 is the initial charge and Q_T is the total charge the battery can store.

E. Planetary Gear System

A PGS is used as the mechanical coupling between the ICE and the EM, as proposed in (Becerra *et al.*, 2011). A schematic is shown in Fig. 4. On this coupling, the ICE output shaft is connected to the sun gear, the EM to the ring gear and the gear box is connected to the carrier gear.

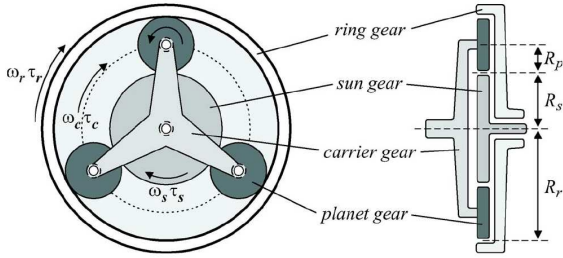


Fig. 4. Planetary Gear System.

With $k = R_r/R_s$, the angular speeds on the PGS satisfy

$$\omega_c = \frac{1}{k+1}\omega_s + \frac{k}{k+1}\omega_r \quad (11)$$

and the balance of power satisfies

$$\tau_c\omega_c = \tau_s\omega_s + \tau_p\omega_p \quad (12)$$

where ω is angular speed, τ is torque and subscripts s , c and p mean sun gear, planet carrier and ring gear, respectively.

III. POWER SPLIT STRATEGY

The problem to be solved, from the optimization point of view, is to minimize the fuel consumption over a desired driving cycle

$$\min J = \int_0^{t_c} \dot{m}_f(\omega_{ice}(t), \tau_{ice}(t)) dt \quad (13)$$

subject to

$$\omega_{ice \min} \leq \omega_{ice}(t) \leq \omega_{ice \max} \quad (14)$$

$$\tau_{ice \min} \leq \tau_{ice}(t) \leq \tau_{ice \max} \quad (15)$$

$$\omega_{em \min} \leq \omega_{em}(t) \leq \omega_{em \max} \quad (16)$$

$$\tau_{em \min} \leq \tau_{em}(t) \leq \tau_{em \max} \quad (17)$$

$$P_{bat \min} \leq P_{bat} \leq P_{bat \max} \quad (18)$$

$$SOC_{\min} \leq SOC(t) \leq SOC_{\max} \quad (19)$$

where subscripts min and max means the minimum and maximum value for the constrained variable and t_c is the duration of the driving cycle.

When the ICE is used, a feasible solution would be to only operate the ICE in the regions where it spends less fuel per power generated, i.e., in the most efficient operation points like in a serial HEV configuration. The strategy proposed in this work is based on this solution.

In addition to keep the ICE on its most efficient region when it is used, the vehicle must follow the driving cycle. In consequence the problem to be solved is to meet the power P_p on the output of the PGS, while the ICE operates on its most efficient region. This problem has multiple solutions, since many combinations of torque and speed at each power source can yield the demanded power P_p (Becerra *et al.*, 2011).

Rewriting Eq. (11) and (12) in terms of the ICE and EM variables, the equations that constraint the solution of this problem are

$$P_p = \tau_p\omega_p = \tau_{ice}\omega_{ice} + \tau_{em}\omega_{em} = P_{em} + P_{ice} \quad (20)$$

$$\omega_p = \frac{1}{k+1}\omega_{ice} + \frac{k}{k+1}\omega_{em} \quad (21)$$

The approach presented on this work is based on the following assumptions:

- 1) The strategy meets the power required to achieve the driving cycle, if it is feasible.
- 2) The ICE operation is optimized in order to operate on its highest efficient power and speed, while possible.
- 3) The EM is used to generate or absorb the lack or excess of power, once the ICE power has been set.
- 4) A PI controller adjusts dynamically the use of the ICE in order to keep the SOC near a given reference.

A block diagram of the proposed strategy is shown in Fig. 5.

A. ICE Power

When $P_p > 0$, the first step of this strategy is to determine a pre-value for the ICE power \hat{P}_{ice} , the final P_{ice} will be set at the end to assure tracking of the driving cycle. In almost all the cases \hat{P}_{ice} will be the final power.

In general, there are only two cases when the ICE should work out from its maximum efficiency operation point $ICE_{eff \max}$, and they are:

- 1) When the required driving cycle power is very low or very high, the ICE should be off or should complement the lack of power, respectively.

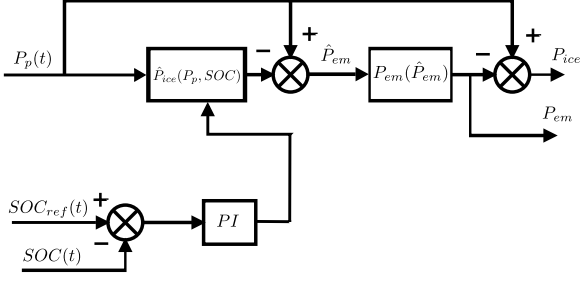


Fig. 5. Strategy Topology.

- 2) When the SOC is not on the given reference, the ICE has to compensate this excess or lack of power.

A solution would be to saturate the ICE when the previous cases occurs, but instead, like in (Becerra *et al.*, 2011), a soft curve is proposed based on the previous observations, it depends on the power required and on the SOC

$$\hat{P}_{ice}(\hat{P}_p, SOC) = \alpha(\hat{P}_p, SOC) P_{ice \max} \quad (22)$$

where \hat{P}_p is the normalized value of P_p defined as $\hat{P}_p = \frac{P_p}{P_{ice \max}}$ and $\alpha(\hat{P}_p, SOC) \in [0, 1]$, defined as

$$\alpha(\hat{P}_p, SOC) = \frac{(2\hat{P}_p + \xi + SOC_{comp}(SOC) - 1)^7}{2} + \frac{P_{ice_eff}}{P_{ice \max}} \quad (23)$$

which ranges between 0 and 1. P_{ice_eff} is the ICE most efficient power and $P_{ice \max}$ is the ICE maximum power. ξ assures that $\alpha(\hat{P}_p, SOC) = 1$ when $P_p = P_{ice \max}$ (or $\hat{P}_p = 1$) and $SOC_{comp} = 0$. For a given P_{ice_eff} and $P_{ice \max}$, ξ is defined as

$$\xi = \sqrt[7]{2(1 - \frac{P_{ice_eff}}{P_{ice \max}})} - 1 \quad (24)$$

SOC_{comp} is the SOC compensator for the P_{ice} . Its role is to move the power calculated in Eq. (23) according to the difference between a reference for the SOC, SOC_{ref} , and the instantaneous SOC, $SOC(t)$. In other words, if $SOC(t)$ is below to SOC_{ref} , more use of the ICE is expected, and if $SOC(t)$ is over SOC_{ref} , less use of the ICE is expected.

Based on the efficiency map, Ec. (23) was designed in order to operate the ICE on its most efficient power, P_{ice_eff} , as much as possible. It could be appreciated on Fig. 6, which shows the plot of $\alpha(\hat{P}_p, SOC)$ with $\frac{P_{ice_eff}}{P_{ice \max}} = 0.5$ and $SOC_{comp} = 0$.

Fig. 7 shows the plot of $\alpha(\hat{P}_p, SOC)$ with several values of SOC_{comp} . It can be seen that, to keep $SOC(t)$ over a desired SOC, positive values are expected when $SOC(t)$ is below to SOC_{ref} , and negative values are expected when $SOC(t)$ is over to SOC_{ref} .

To achieve this behavior of SOC_{comp} , a PI controller is used in order to keep the SOC around a given reference. This controller is necessary because without it the strategy

tends to fill up or to deplete the battery, depending on the driving cycle. The SOC compensator SOC_{comp} is defined as follows

$$SOC_{comp}(SOC) = k_p (SOC_{ref} - SOC(t)) + k_i \int_0^t (SOC_{ref} - SOC(\tau)) d\tau \quad (25)$$

where k_i and k_p are the tuning parameters for the PI controller.

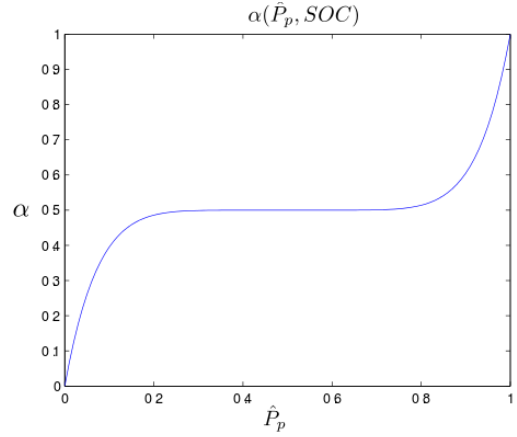


Fig. 6. Plot of $\alpha(\hat{P}_p, SOC)$.

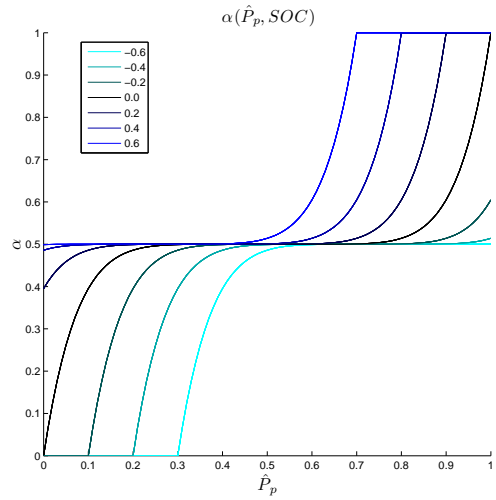


Fig. 7. Plot of $\alpha(\hat{P}_p, SOC)$ for several values of SOC_{comp} .

At this point, a first proposal for the ICE power could be calculated, but the final P_{ice} is calculated after the EM power is set, to assure meeting the requested power, as illustrated in Fig. 5. Setting of EM power is explained later on. The final value for P_{ice} is

$$P_{ice} = \max(\hat{P}_{ice}, P_p - P_{em}) \quad (26)$$

which is saturated between 0 and $P_{ice \max}$.

When P_{ice} has been set, ω_{ice} and τ_{ice} need to be found. Taking advantage of the cinematic relation of the PGS, expressed on Eq. (20), ω_{ice} can be set to achieve the maximum efficiency for the ICE at a given power. The algorithm presented in the next section is used for this purpose. Finally, the ICE torque is set with

$$\tau_{ice} = \begin{cases} 0 & \text{for } \omega_{ice} = 0 \\ \frac{P_{ice}}{\omega_{ice}} & \text{for } \omega_{ice} > 0 \end{cases} \quad (27)$$

ICE Speed Optimization: In this section an algorithm to find the most efficient ICE speed, for a given power, using an efficiency map is presented.

Once P_{ice} has been set, it is necessary to determine the ICE speed ω_{ice} in order to find the solution to Eqs. (20) and (21). In (Becerra *et al.*, 2011) ω_{ice} is found using information given by the ICE manufacturer. This information is not always available, instead efficiency maps, presented as a table, are used by most simulation tools (Markel *et al.*, 2002)(Gao *et al.*, 2007).

Given a table ICE_{map} that maps ω_{ice} and τ_{ice} with an ICE efficiency, $ICE_{eff}(\omega_{ice}, \tau_{ice})$, the next algorithm can be applied:

- 1) Start with the lowest P_{ice} , minimum ω_{ice} and τ_{ice} , in the table ICE_{map} , and take it as base power P_{base} , and its corresponding ω_{base} and τ_{base} , for the first iteration.
- 2) Search on ICE_{map} the biggest neighbor to P_{base} (by increasing ω_{base} or τ_{base}) that offers the highest $\Delta ICE_{eff} / \Delta P_{ice}$ with respect to P_{base} .
- 3) Add the found power in step 2, and its corresponding speed, to the table $\omega_{ice-eff}$.
- 4) Take as the new P_{base} the power found in step 2, and its corresponding ω_{base} and τ_{base} .
- 5) Repeat from step 2 until the maximum power from table ICE_{map} is reached.
- 6) The table generated in step 3 maps a given power to its most efficient speed, in other words, it generates $\omega_{ice-eff}(P_{ice})$.

Fig. 8 shows the plot of P_{ice} vs ICE_{eff} at a constant speed for the speeds defined in ICE_{map} . The upper contour is the plot of the table $\omega_{ice-eff}(P_{ice})$ found with the previous algorithm for the ICE that was chosen for simulations on this work. The plot of P_{ice} vs $\omega_{ice-eff}(P_{ice})$ is shown in Fig. 9.

B. EM Power

It is expected that the EM compensates the difference between P_p and P_{ice} in order to meet the required power, although it is limited by the EM maximum and minimum power $P_{em,max}$ and $P_{em,min}$. As it is shown in Fig. 5, a pre-value for the EM power is

$$\hat{P}_{em} = P_p - \hat{P}_{ice} \quad (28)$$

and the final value for the EM power is

$$P_{em}(\hat{P}_{em}) = \max\left(P_{em,min}, \min\left(P_{em,max}, \hat{P}_{em}\right)\right) \quad (29)$$

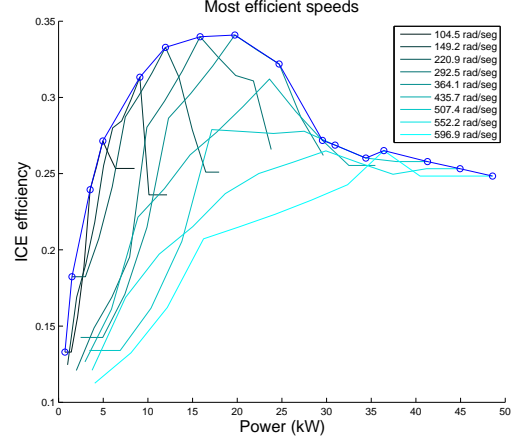


Fig. 8. ICE power vs efficiency at constant speed.

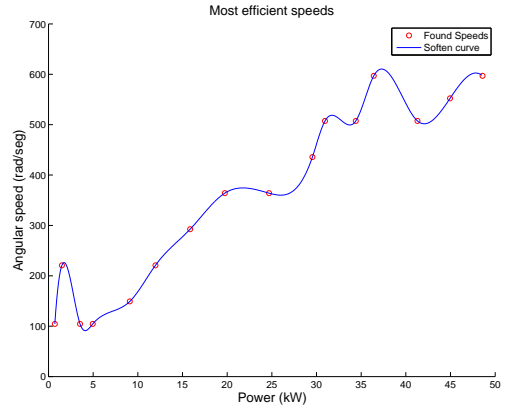


Fig. 9. ICE power vs efficient speed.

Finally, from Eq. (20), EM speed and torque are calculated

$$\omega_{em} = \frac{k+1}{k} \left(\omega_p - \frac{\omega_{ice}}{k+1} \right) \quad (30)$$

$$\tau_{em} = \begin{cases} 0 & \text{for } \omega_{em} = 0 \\ \frac{P_{em}}{\omega_{em}} & \text{for } \omega_{em} \neq 0 \end{cases} \quad (31)$$

C. Regenerative Braking

In case of braking $P_p < 0$, it is necessary to recover as much energy as possible, taking care of not damaging the batteries (Becerra *et al.*, 2011). In this case $P_{ice} = 0$ and P_{em} is

$$P_{em}(SOC) = \max(P_p, \beta(SOC)P_{em,max}) \quad (32)$$

with

$$\beta(SOC) = 0.5 [\tanh(A_1(SOC - SOC_{max}))] - 0.5 \quad (33)$$

where A_1 is a design parameter. Fig. 10 shows the plot of β with $A_1 = 0.8$ and $SOC_{max} = 90\%$.

Finally, the required power at friction brakes is

$$P_f = P_p - P_{em} \quad (34)$$

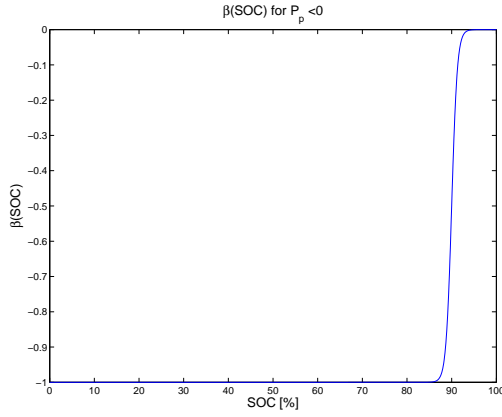


Fig. 10. Regenerative braking power in function of SOC.

IV. SIMULATION RESULTS

On this section, results of simulating on ADVISOR the vehicle and the strategy presented on the previous sections on ADVISOR are shown. To get an idea of the strategy performance, it is compared against a rule based strategy with the same vehicle parameters but without the PGS. Main parameters for the simulated vehicle are shown in Table I.

Total mass	912 kg
ICE power	41 kW
Li-Ion Battery, 6 Ah and $V_{nom} = 267V$	25 kW
EM power	25 kW
Gear box	5 speeds

TABLE I

MAIN PARAMETERS FOR THE SIMULATED VEHICLES.

Strategy parameters are shown in Table II. ICE_{map} was taken from the ADVISOR database.

SOC_{ref}	70%
SOC_{max}	85 %
A_1	1
k (PGS ratio)	5
$P_{ice-eff}$	20kW
$P_{ice-max}$	41kW
k_p	1
k_i	0.01

TABLE II

POWER SPLIT STRATEGY PARAMETERS.

Table III shows the fuel consumption from the presented strategy for two driving cycles, simulations are shown in Figs. 11 and 12. Table IV shows the fuel consumption for the same driving cycles when a rules based strategy is used

and simulation results for this rules based strategy are shown in Figs. 13 and 14.

It is convenient to emphasize that initial SOC on simulations where set, after several trials, to coincide with the final SOC. Taking this in consideration, the fuel consumption is only due to the power split strategy used to move the vehicle and not affected by the electrical storage system and gives a clear picture about the strategy performance. It is evident that there is a great improvement with the proposed strategy, specially on urban conditions.

Cycle	Initial SOC (%)	Final SOC (%)	Fuel Consumption (L/100 km)
UDDS	71.14	71.14	4.2996
HWFET	70.72	70.72	4.3169

TABLE III

SIMULATION RESULTS FOR THE VIRTUAL SERIAL STRATEGY.

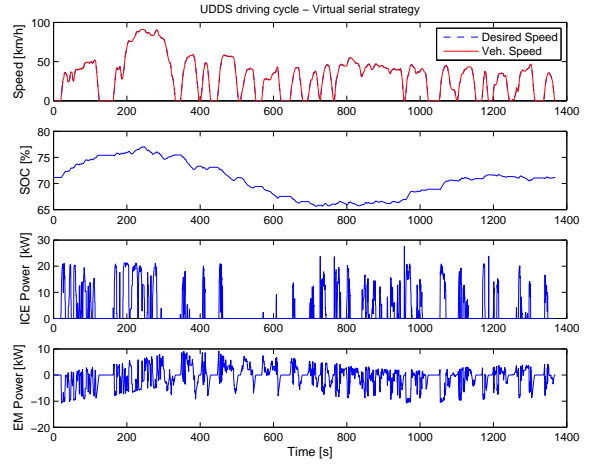


Fig. 11. Virtual Serial Strategy over UDDS cycle.

Cycle	Initial SOC (%)	Final SOC (%)	Fuel Consumption (L/100 km)
UDDS	69.66	69.66	6.5246
HWFET	71.5	71.5	4.8696

TABLE IV

SIMULATION RESULTS FOR THE RULES BASED STRATEGY.

In Figs. 11 and 12 it can be appreciated that the ICE works always around its more efficient power, 19.7kW. This is confirmed in Figs. 15 and 16, that shows ICE efficiency histograms ($P_{ice} > 0$) for UDDS and HWFET cycles.

V. CONCLUSIONS

In this work a new strategy for HEV has been proposed. It is supported by an innovative way to couple the power sources presented in (Becerra *et al.*, 2011). Although It is not proven to be optimal, it is inspired on optimal control

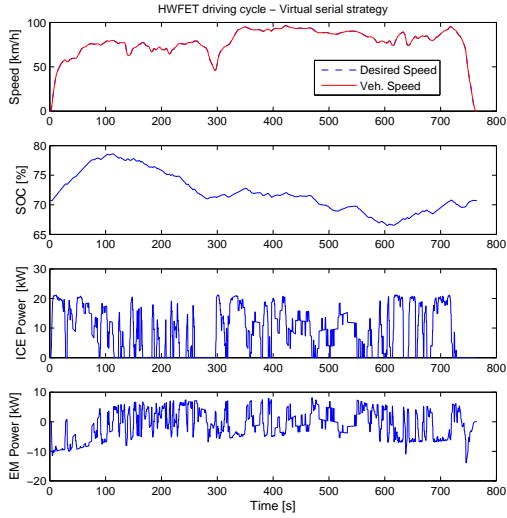


Fig. 12. Virtual Serial Strategy over HWFET cycle.

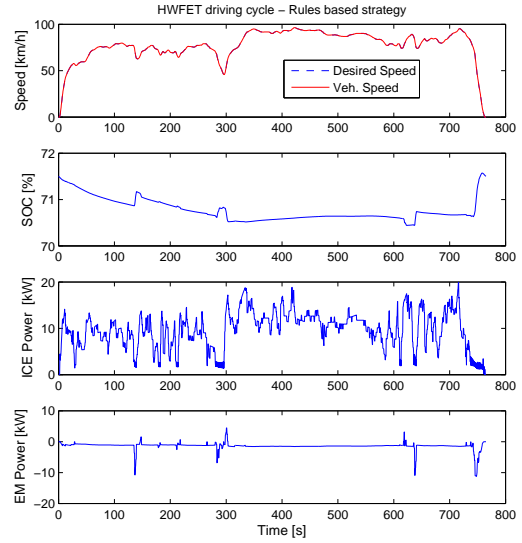


Fig. 14. Rules based strategy over HWFET cycle

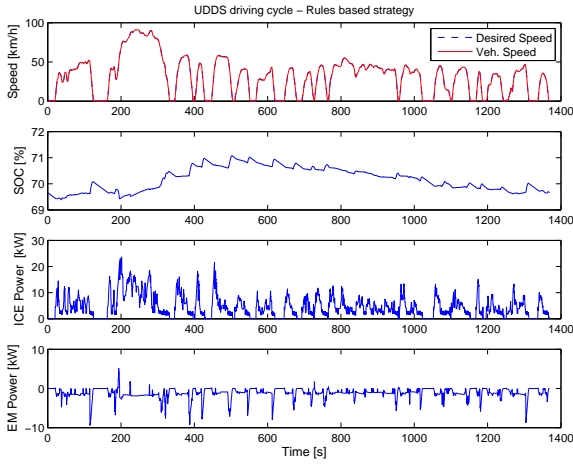


Fig. 13. Rules based strategy over UDSS cycle

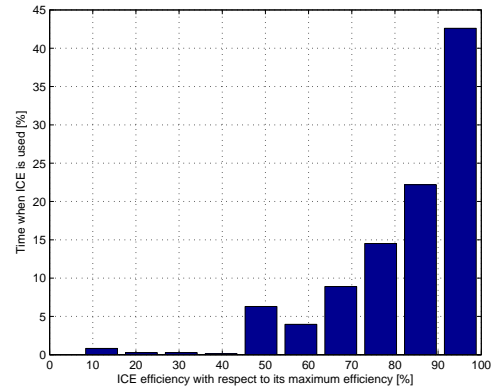


Fig. 15. ICE efficiency histogram when ICE is used in cycle UDSS.

theory. Furthermore, a procedure is given to optimize the ICE speed given a ICE power. The proposed strategy has the advantage of being easy to implement as it has low computational requirements, compared with other approaches.

The strategy operates the ICE on its most efficient region and a PI controller is used to compensate the deviation of the SOC. This compensator has the advantage of being easy to tune since, basically, it depends only in two parameters, which are the main parameters for the strategy. Although in this work a PI controller was used, other controllers could be used.

Simulation results show the performance of the strategy compared with a rules based strategy. They also show that, effectively, the ICE operates on around its most efficient region. Also, results demonstrate that the strategy is robust, from the driving cycle point of view, since it shows good

performance for urban conditions as for highway conditions.

A. Future Work

There are several topics that are opened on this work:

- 1) Prove the optimality of the strategy or under which conditions it is optimal.
- 2) Compare the strategy with the DP solution as a way to evaluate its performance.
- 3) Study the effect of having *a priori* information of the driving cycle on the performance of the strategy.
- 4) Study the effect of the strategy on the dimensioning of the HEV power sources (ICE, EM and battery).
- 5) Test the performance of the strategy with other controllers for the SOC compensator instead of the PI controller.

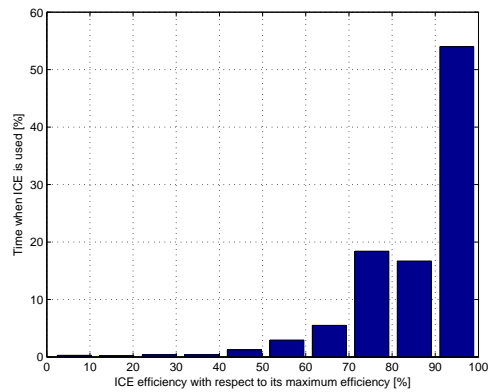


Fig. 16. ICE efficiency histogram when ICE is used in cycle HWFET.

ACKNOWLEDGMENT

Research was supported by CONACYT 103640 and UNAM-PAPIIT IN105512 grants.

REFERENCES

- Becerra, Guillermo, Jose Luis Mendoza-Soto y Luis Alvarez-Icaza (2011). Power flow control in hybrid electric vehicles. *Proceedings of The 4th Annual Dynamic Systems and Control Conference*.
- Borhan, H.A., A. Vahidi, A.M. Phillips, M.L. Kuang y I.V. Kolmanovsky (2009). Predictive energy management of a power-split hybrid electric vehicle. En: *American Control Conference, 2009. ACC '09*. pp. 3970 –3976.
- Delprat, S., T.M. Guerra, G. Paganelli, J. Lauber y M. Delhom (2001). Control strategy optimization for an hybrid parallel powertrain. En: *American Control Conference, 2001. Proceedings of the 2001*. Vol. 2. pp. 1315 –1320 vol.2.
- Delprat, Sebastien, Jimmy Lauber, Thierry Marie Guerra y J. Rimaux (2004). Control of a parallel hybrid powertrain: optimal control. *IEEE Transactions on Vehicular Technology* **Vol. 53**(3), 872–881.
- Gao, D.W., C. Mi y A. Emadi (2007). Modeling and simulation of electric and hybrid vehicles. *Proceedings of the IEEE* **95**(4), 729 –745.
- Gong, Qiuming, Yaoyu Li y Zhong-Ren Peng (2008). Trip-based optimal power management of plug-in hybrid electric vehicles. *Vehicular Technology, IEEE Transactions on* **57**(6), 3393 –3401.
- Johannesson, Lars y Bo Egardt (2008). Approximate dynamic programming applied to parallel hybrid powertrains. *Proceedings of the 17th IFAC World Congress*.
- Kessels, John T. B. A., Michiel W. T. Koot, Paul P. J. van den Bosch y Daniel B. Kok (2008). Online energy management for hybrid electric vehicles. *Vehicular Technology, IEEE Transactions on* **57**(6), 3428 – 3440.
- Langari, R. y Jong-Seob Won (2003). Integrated drive cycle analysis for fuzzy logic based energy management in hybrid vehicles. En: *Fuzzy Systems, 2003. FUZZ '03. The 12th IEEE International Conference on*. Vol. 1. pp. 290 – 295 vol.1.
- Lin, Chan-Chiao, Huei Peng, J.W. Grizzle y Jun-Mo Kang (2003). Power management strategy for a parallel hybrid electric truck. *Control Systems Technology, IEEE Transactions on* **11**(6), 839 – 849.
- Lin, Chan-Chiao, Huei Peng, Soonil Jeon y Jang Moo Lee (2002). Control of a hybrid electric truck based on driving pattern recognition. *Proceedings of the 2002 Advanced Vehicle Control Conference*.
- Markel, T. A Brooker, T Hendricks, V Johnson, K Kelly, B Kramer, M OKeefe, S Sprik y K Wipke (2002). Advisor: a systems analysis tool for advanced vehicle modeling. *Journal of Power Sources* **110**(2), 255 – 266.
- Musardo, C., G. Rizzoni y B. Staccia (2005). A-ecms: An adaptive algorithm for hybrid electric vehicle energy management. En: *Decision and Control, 2005 and 2005 European Control Conference. CDC-ECC '05. 44th IEEE Conference on*. pp. 1816 – 1823.
- Schouten, Niels J., Mutasim A. Salman y Naim A. Kheir (2002). Fuzzy logic control for parallel hybrid vehicles. *IEEE Transactions on Vehicular Technology* **Vol. 10**, 460–468.
- Sciarretta, A., M. Back y L. Guzzella (2004). Optimal control of parallel hybrid electric vehicles. *Control Systems Technology, IEEE Transactions on* **12**(3), 352 – 363.
- van Keulen, T., B. de Jager, A. Serrarens y M. Steinbuch (2010). Optimal energy management in hybrid electric trucks using route information. *Oil & Gas Science and Technology* **65**(1), 103–113.
- Zhang, Chen, Ardalan Vahidi, Pierluigi Pisu, Xiaopeng Li y Keith Tennant (2010). Role of terrain preview in energy management of hybrid electric vehicles. *IEEE Trans. Veh. Technol* **59**(3), 1139–1147.
- Zhang, Xiangqun, Jack Katzberg, Bruce Cooke y J.Kos (1997). Modeling and simulation of a hybrid-engine. *Conference on Communications, Power and Computing, Winnipeg, MB* pp. 286–291.